Author's Accepted Manuscript

Interpreting the Effects of Interfacial Chemistry on the Tribology of Diamond-Like Carbon Coatings against Steel in Distilled Water

D.C. Sutton, G. Limbert, B. Burdett, R.J.K. Wood

Interpreting the Effects of Interfacial Chemistry on the Tribology of Diamond-Like Carbon Coatings against Steel in Distilled Water

D. C. Sutton[*1], *G. Limbert*[1], *B. Burdett*[2], *R.J.K. Wood*[1]

[1]*National Centre for Advanced Tribology, University of Southampton, SO17 1BJ, UK;*
[2]*Materials Specialist, Rolls Royce Submarines.*
Email Address: ds6c10@soton.ac.uk; Tel: +44 2380 597667

Three commercially available Diamond-Like Carbon (DLC) coatings were investigated to help understand the dynamics of transfer layer formation and decay, when sliding against AISI 52100 steel balls in distilled water. Optimum tribological behaviour was observed during interfacial sliding between the transfer layer and DLC coating. Alternatively, shear of the carbonaceous transfer layer from the contact region resulted in growth of an iron oxide layer comprised of magnetite, maghemite and hematite, as identified by Raman spectra. Three-body abrasive wear involving iron oxide wear particles explained the high wear rate of the DLC coatings in the case of shear.

Friction was controlled by the formation of a transfer layer, reducing adhesive interactions between surfaces. Subsequently, a gradual increase in friction was observed, and suggested to relate to an increase in the shear strength of the transfer layer due to adsorption of oxidative species. This was modelled using the Elovich equation for gas adsorption kinetics.

Keywords: Friction modelling; DLC coating; Transfer layer; Iron oxide; Raman spectroscopy; Water.

1. Introduction

Diamond-Like Carbon (DLC) coatings can provide low friction and wear behaviour in a wide range of applications, due to their excellent mechanical and tribological properties [1-3]. Advanced coating deposition techniques such as Chemical Vapour Deposition (CVD) can provide application-specific solutions to minimise friction or wear whilst preserving macroscopic engineering tolerances. These coatings display differing tribological behaviour depending on their chemical composition and mechanical properties.

Importantly, the tribology of DLC coatings is affected by the surrounding environment, which adds complexity to the estimation of a coatings lifetime. There exists a need to understand the mechanical and chemical processes that occur in a tribo-contact, in order to eventually enhance the long-term survival of a coating in a specific application. Understanding of the dynamics of transfer layer growth and decay is vital to this.

It is well documented that during the sliding contact of a DLC coating and a counterface material, typically, a transfer layer forms on the counterface [2]. In general, a transfer layer is composed of disordered carbon wear debris from the DLC coating, as well as wear debris from the counterface, and any reactive environmental species [4]. This solid lubricant layer acts to control frictional behaviour, and lower wear.

The effect of water vapour on the tribology of DLC coatings has been observed by numerous authors [5-7]. In dry sliding, hydrogenated DLC coatings typically show a coefficient of friction in the range 0.01 − 0.1 and extremely low wear rates below 10^{-8} mm^3/Nm. Introduction of water vapour causes an increase in friction and wear. Non-hydrogenated coatings can show high friction above 0.5 in dry sliding, but show reduced friction and wear due to the formation of low energy surfaces by adsorption of environmental species in the presence of water vapour [7].

The dependence of the coefficient of friction of DLC coatings on the environment has been modelled previously using the Elovich equation for gas adsorption [8-11]. The fractional coverage of the surface by adsorbed molecules θ can be described according to Equation 1.

$$\frac{d\theta}{dt} = Be^{-\alpha\theta} \tag{1}$$

In Equation 1, α is a constant that controls the rate of adsorption, and B is the initial rate of adsorption, and can be generalised to include effects of pressure and temperature. The adsorption of environmental species onto the surface of DLC coatings was shown to be reversible, and to strongly influence the coefficient of friction. Dickrell et al. [12-14] used a Langmuir adsorption model to consider the effects of temperature and humidity on the rate of adsorption. The rate of desorption, due to mechanical sliding, was included in the model.

The tribology of DLC coatings is dependent not only on the environment, but also on the composition of the counterface. Park et al. [15] examined the tribology between a steel ball and a hydrogenated DLC coating in a

2

humid environment. A high coefficient of friction was observed, and was related to oxidation of the steel ball resulting in Fe-rich wear debris. Similarly, Uchidate et al. [16] observed a transfer layer containing mainly of Fe, O, and C when sliding in water, as a result of tribochemical reactions between surfaces.

Li et al. [4] proposed that adhesive interactions between a DLC coating and steel ball in the presence of humidity were due to oxidation of the DLC coating surface, and chemical reactions between the DLC coating and steel ball. X-ray Photoelectron Spectroscopy (XPS) showed the presence of $C - O$ and $C = O$ bonding on the DLC coating surface, as well as $Fe - C$ bonding in high humidity. Previous works [1, 17, 18] have quoted the bonding energy for a $C - H$ bond was calculated to be 0.08 eV, compared to 0.21 eV per bond for $C - O$ and $C = O$ bonds, which explains the increase that was observed in friction.

However, the tribology of DLC coatings is dependent on the deposition method, and Wu et al. [19] showed a low coefficient of friction for hydrogenated DLC coatings deposited by a thermal electron plasma CVD method in a water environment. Using a stable isotopic tracer, they confirmed oxidation of the DLC coating surface by tribochemical reactions with water when sliding against steel, and related the low coefficient of friction to the formation of hydroxyl and carboxyl groups on the DLC coating surface, leading to hydrophilic behaviour that promoted low friction. This is very different tribological behaviour from that observed in the work of Li et al. [4], and suggests that there are other important factors involved.

The sensitivity in tribological behaviour may be related to the type of interfacial motion at the interface between surfaces. Recently, Scharf and Singer [20] have shown, via *in situ* Raman spectroscopy, the formation of a transfer layer in the tribo-contact occurs in the first few cycles via third body processes. For W-DLC in humid air, a transfer layer was observed to grow across the contact region, and interfacial sliding occurred between the transfer layer and the DLC coating resulting in low wear. Conversely, in dry air the thinning then removal of material caused high variance in the coefficient of friction and increased wear. Shearing and re-attachment of third-body material was observed.

Further study to better understand the transfer layer growth and decay, for DLC coatings sliding against steel in distilled water, are important to industry. Of note is a need for greater understanding of the chemical processes that occur in a DLC contact, in order to allow for prediction of the dynamics of transfer layer growth and decay, and ultimately the life behaviour of the coating.

3

This paper examines the tribology of three DLC coatings in distilled water against 52100 steel balls. Firstly, sliding wear tests were performed for each coating over a range of test times. The effects of shear on the friction and wear, and the evolution of the transfer layer as a result, were investigated. Raman spectroscopy was used to determine the interfacial chemistry at various stages throughout the tests. The second section of this paper links the interfacial chemistry with the frictional behaviour observed in the laboratory, by means of an Elovich adsorption model.

2. Materials and methods

2.1. Wear testing of the DLC coatings

2.1.1. Mechanical categorisation

Three commercially available DLC coatings were deposited onto AISI 4118H low-alloy steel disks of 0.1 μm average roughness, and 7.5 GPa hardness. Coating A is a chromium-doped magnetron sputtered coating produced using a closed field unbalanced magnetron sputter ion plating (CFUBMSIP) system with two carbon and two chromium targets. A chromium interlayer followed by a chromium – carbon gradient layer maximises adhesion. Coating B is a metal-free hydrogenated DLC coating produced though a plasma-enhanced CVD (PECVD) method. A chromium nitride interlayer is used to enhance adhesion and provide load support. Coating C is a hydrogenated PECVD deposited DLC coating at extremely low temperature (< 100°C) resulting in lower thermal stresses. Since all coatings used in this work are commercial, detailed knowledge of deposition processes is unknown. The mechanical properties for the DLC coatings are given in Table 1.

Table 1: Deposition, composition, and mechanical properties of the DLC coatings

	Coating A	Coating B	Coating C
Deposition Method	CFUBMSIP	PECVD	PECVD
Coating Layers	a-C/Cr:C/Cr	a-C:H/CrN	a-C:H
Bonding Type	Primarily sp^2	Primarily sp^3	Primarily sp^3
Roughness, R_a	0.097 μm	0.098 μm	0.075 μm
Coating Thickness	1.5 μm	1.4 μm	6 μm
Hardness, H	13.1 (± 1.1) GPa	20.1 (± 2.7) GPa	21.3 (± 0.6) GPa
Elastic Modulus, E	155 (± 9.1) GPa	212 (± 17.2) GPa	191 (± 2.5) GPa
H/E	0.085	0.095	0.112

All coatings are dark grey in colour. On coating A and B, scratches from the underlying substrate are evident due to the conformity of the thin coating and the substrate. There are defects visible on the surface which are relics from deposition, and go most or all of the way through the coating, as analysed by surface profilometry. Coating C is smoother than the other coatings at 0.075 μm average roughness, and near featureless, although some defects are present.

2.1.2. Nanoindentation

Mechanical properties of the DLC coatings were measured on a NanoTest platform (Micro Materials Limited, Wrexham, UK). Nanoindentations were performed using a Berkovich indenter, and trial testing was performed to identify suitable load/depth for the indents. Indentations were typically 100 nm for coatings A and B, and 300 nm for coating C due to its higher thickness. Indentations to peak loads of 3 – 6 mN were performed over 20 seconds of loading time, held for 2 seconds, and then unloaded over 20 seconds. Thermal drift corrections were performed pre- and post-indent. Relatively high surface roughness caused some scatter in the response for coatings A and B, however coating C showed impressive mechanical consistency over a range of loads.

Table 1 lists the mechanical properties of the DLC coatings. Coating A showed a hardness of 13.1 GPa, which is softer than coating B and C, which were 20.1 GPa and 21.3 GPa respectively. The hardness of DLC coatings is known to increase with sp^3 content [3], and coating A is known to have lower sp^3 content that coating B and C. Assuming a Poisson's ratio of 0.22 [21], elastic moduli were calculated from the measured reduced moduli. Coating A displayed an elastic modulus of 155 GPa in comparison to coatings B and C which showed 212 GPa and 191 GPa, respectively.

2.1.3. Reciprocating ball-on-flat experimental set-up

DLC coatings were cleaned in an cleansing detergent (Ultraclean M2, Ultrawave Ltd, Cardiff, UK) in an ultrasonic bath for 20 minutes, before rinsing in distilled tap water, and cleaning two more times in the ultrasonic bath in fresh distilled tap water for ten minutes each. The DLC coatings were immersed immediately in distilled tap water in the rigs reservoir.

The dynamic friction was measured using a Plint TE77 reciprocating tribometer (Phoenix Tribology Ltd, Newbury, UK). A ball-on-flat configuration was chosen (see Figure 1), and 6 mm diameter 52100 balls of 0.1 μm average surface roughness were used as a counterface. The coatings were tested using a 5 N load, to

simulate a 1 GPa maximum contact pressure (estimated using the DLC elastic properties). A 19 mm stroke at a frequency of 2 Hz gave an average sliding speed of 0.076 m s^{-1}. Friction tests were performed for 30, 120, and 600 seconds, relating to a sliding distance of 2.3 m, 9.1 m, and 45.6 m. Contact potential measurements and bulk temperature were also continuously recorded. In each case two tests were performed to judge repeatability.

Wear depths of the 52100 steel balls were evaluated analytically using the known ball radius, and wear volume measurements from an Alicona InfiniteFocus (Alicona Imagine GmbH, Graz, Austria) surface profilometer, to a resolution of 20 nm. The wear depths of the DLC coatings were measured similarly on the Alicona InfiniteFocus surface profilometer, based on wear volume measurements divided by the area of the wear scar.
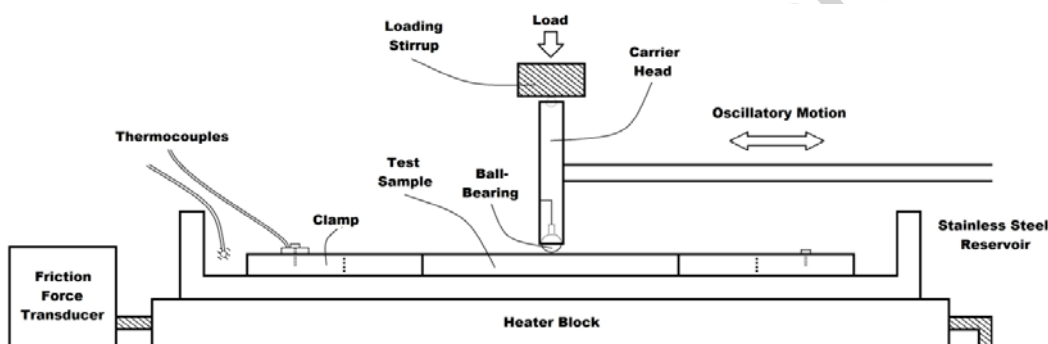
Figure 1: TE77 test configuration.

Analysis of transfer layers was performed using a JSM 6500 Scanning Electron Microscopy (SEM). Backscatter Electron Imaging (BEI) and Electron Dispersive X-ray (EDX) chemical mapping were used.

2.2. Raman spectroscopy

Raman spectroscopy was performed on a Renishaw spectrometer (National Physics Laboratory, Teddington, UK) with a 514 nm laser using a 1 μm spot-size. The spectra were recorded at room temperature over a range of 100 – 2000 cm^{-1} and an operating power of 4 mW. The acquisition time was 10 seconds.

2.3. A friction model for oxidation of wear debris

Increased friction of DLC coatings has previously been observed in a water environment [17]. As humidity increases the frictional behaviour becomes environmentally dependent, as opposed to being intrinsically related to the composition of the DLC coating. Increases in the coefficient of friction due to adsorption phenomena have been modelled for DLC coatings sliding in vacuum and exposed to ambient air [9, 10]. In the

6

case of DLC sliding in water, we can use a similar approach and apply this adsorbate model to the chemical adsorption of polar species onto the wear debris at the interface.

For material to wear from the DLC coating, the carbon matrix must be mechanically broken, producing macro-radicals which will react with environmental species present [4]. In the case of sliding in distilled water, these macro-radicals will react with water and oxygen molecules, leading to oxidation of the DLC coating surface, or the production of oxidised wear debris. An increase in adhesive friction will follow as a result these reactions. Additionally, the formation of various iron oxides will occur from reaction on water with Fe, leading to enhanced wear to the steel ball. Further friction-induced oxidation may occur within the transfer layer.

The coefficient of friction is determined by the shear strength of the wear debris in the contact, and the real area of contact. Assuming that the normal load N is supported on this area, we find that the friction can be calculated by Equation 2 [22].

$$\mu = \frac{F_N}{N} = \frac{\tau}{P} \tag{2}$$

The interfacial shear strength τ will vary according to the chemistry of the wear debris. Additionally, the interfacial shear strength varies according to the amount of the debris in the contact. If there is not enough transfer layer present in the contact region then asperity contacts may occur between the DLC coating and steel ball, causing an increase in shear strength. Additionally, for initially high wear, a lot of wear debris might cause an initially large contribution to friction. This is due to the mechanical work that is needed to shear the debris from the contact.

Heimberg et al. [10] were the first to use the Elovich equation in the context of DLC coatings. A linear relation between the coefficient of friction and the surface coverage of adsorbates was assumed.

$$\mu = \mu_0 + \theta(t)(\mu_1 - \mu_0) \tag{3}$$

In Equation 3, the maximum coefficient of friction is μ_1, and the minimum coefficient of friction is μ_0. The fractional coverage of adsorbate θ can be thought of as a ratio of the number of sites where oxidation has occurred to the total number of potential sites for oxidation to occur. As time continues, θ will increase

7

monotonically as the debris oxidises, to a maximum value of 1 (i.e. 100%). The model assumes constant pressure and temperature, in assuming a constant value for α.

An analytic solution to the Elovich equation exists, assuming $\theta = 0$ at $t = 0$, suggesting the coefficient of friction varies according to Equation 4 [11].

$$\mu(t) = \mu_0 + \frac{\mu_1 - \mu_0}{\alpha} \ln(1 + B\alpha t) \qquad (4)$$

The second important factor in evaluation of the coefficient of friction is the type of interfacial motion. In the case of interfacial sliding, the oxidation of wear debris will increase the adhesive component of friction; however the coefficient of friction will remain low and steady throughout the test. In the case of shear and recirculation of debris in the contact, the coefficient of friction will vary according to the amount of wear debris in the contact. To account for this, we assume a linear wear rate to the transfer layer, causing a linear decrease in the coefficient of friction by assumption. Equation 5 is used to model the time dependency of the coefficient of friction.

$$\mu(t) = \mu_0 + \frac{\mu_1 - \mu_0}{\alpha} \ln(1 + B\alpha t) \frac{h_{max} - kt}{h_{max}} \qquad (5)$$

In Equation 5, h_{max} is the maximum height of the transfer layer. A linear wear rate k describes the evolution in the height of the transfer layer through time. MatLab (MathWorks, Cambridge, UK) was used to optimise the values of α, B, and k/h_{max} to provide the best fit for the model by minimising the residual error between the Elovich model in Equation 5 and the experimental data points.

3. Results and discussion

3.1. Friction and wear

Figure 2 (a) shows the evolution of the coefficients of friction of each coating during a 600 second test in distilled water. The coefficients of friction observed in this work are typical for DLC coatings in a water environment [16, 23]. Coating A has an initially large coefficient of friction due to strong adhesion between the surfaces as a result of the high proportion of sp^2 bonding, and lack of hydrogen in the coating. The surface is composed of clusters of sp^2 bonded carbon, formed of cleavage-faces with low surface energy, and edge-faces

with a high surface energy. The edge-faces are very reactive and high adhesion with the steel surface is experienced as a result. If a DLC coating is hydrogenated, then the surface does not suffer these adhesive interactions by the hydrogen passivation mechanism explained by Erdemir [6]. As the test continues, the friction decreases to 0.23. This was shown to be highly repeatable behaviour via multiple tests. The fall in friction occurs as a transfer layer forms in the contact composed of worn debris from the DLC coating and steel ball. The mechanism for this has been described by Scharf and Singer [20, 24]. The coefficient of friction increases again as the wear debris reacts with oxidative species in the environment, resulting in higher adhesion.

Coatings B and C show relatively steady coefficients of friction in the short test in Figure 2 (a). This is due to their higher hardness, a result of their sp^3 bonding, and their hydrogen content which provides low surface energy by a hydrogen passivation mechanism [6]. Coating C displayed the lowest coefficient of friction of 0.14, which increases slightly to 0.17 throughout the test. Coating C experiences small variance in the coefficient of friction comparative to the other coatings tested. This is due in part to the lower surface roughness.

(a)

(b)
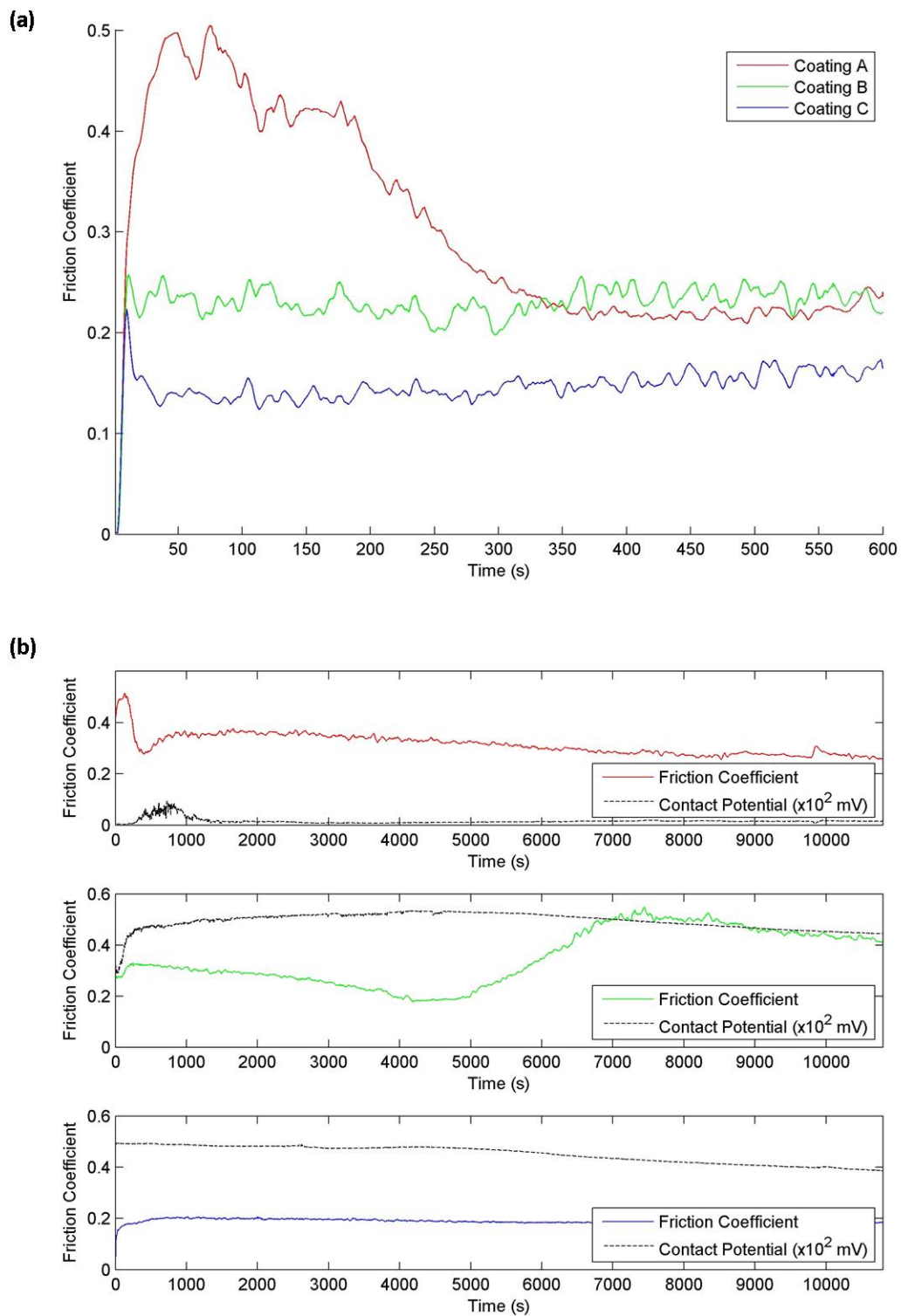
Figure 2: Coefficient of friction of coatings A, B, and C against 52100 steel in distilled water for (a) 600 seconds test time, and (b) 3 hours test time.

The longer frictional tests in Figure 2 (b) for coating A show an initially high frictional force, followed by a decrease in the coefficient of friction as the surfaces wear and a transfer layer forms. The contact potential confirms the presence of a non-conducting layer in the contact. An increase in the coefficient of friction occurs due to the shear-induced reaction of the wear debris with environmental species. Following this, Coating A shows a decreasing coefficient of friction. Coating B shows an initial increase in friction, followed by a steadily decreasing coefficient of friction to a minimum of 0.20. Initially, the contact potential increases dramatically as wear debris is sheared in the contact, then gradually increases as a non-conducting layer grows in the contact. After approximately 80 minutes of sliding, there is a sudden increase in the coefficient of friction. This transition is observed in the work of Uchidate et al. [16] for hydrogenated DLC coatings also, and is unexplained, although we theorise that high adhesion occurs between the DLC coating and steel ball. A similar increase in friction is observed in the work of Fontaine et al. [25] for hydrogenated DLC coatings sliding in UHV. The transfer layer is thought to wear away during this period, resulting in adhesive interactions between steel ball and the DLC coating, and this theory is backed-up by the subsequent decline in the contact potential measurements in Figure 2 (b). Coating C shows an initial increase in the coefficient of friction, followed by very smooth frictional behaviour throughout the rest of the test. Again, the gradual increase in the coefficient of friction is related to the oxidation of worn debris by friction-induced shear.

The wear depth for each DLC coating is shown in Figure 3 (a). A large proportion of the wear occurs during the first 30 seconds of testing, due to an initially high contact pressure and non-conformal surfaces. Coatings A and B showed very similar wear depth, resulting in specific wear rates of 1.7×10^{-6} mm^3/Nm and 2.2×10^{-6} mm^3/Nm, respectively. No wear was measurable for coating C which showed extreme wear resistance, suggesting a specific wear rate of order 10^{-8} mm^3/Nm. The steel balls displayed much higher wear than their DLC counterparts; see Figure 3 (b). Coating B displayed the highest wear depth, whereas coating A and coating C showed similar wear characteristics. It has been observed previously that the wear rate of a counterface in water is dependent on the hardness of the DLC coating [17], and so the relatively low wear depth of coating C in comparison to coating B is surprising. This can be explained however by the formation of a protective transfer layer. Figure 4 shows the ball surfaces after 30, 120, and 600 seconds of wear against each DLC coating. Coating C shows a stable transfer layer at all test times. Little evidence of shear of debris from the region was observed. This correlates with the low and stable coefficient of friction observed for this coating.

11
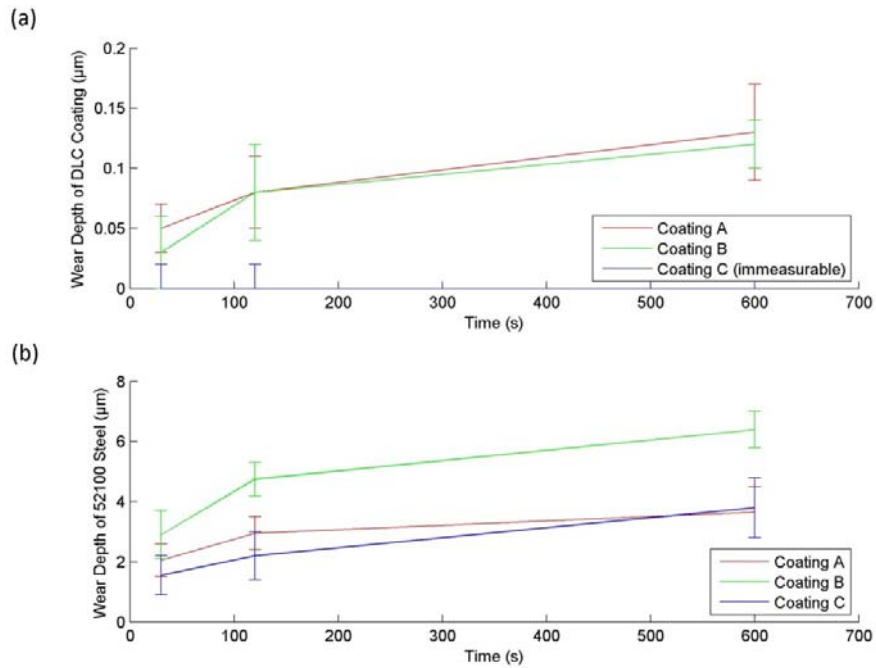
Figure 3: Average wear depth of (a) coatings A, B, and C and (b) 52100 steel in distilled water versus time.
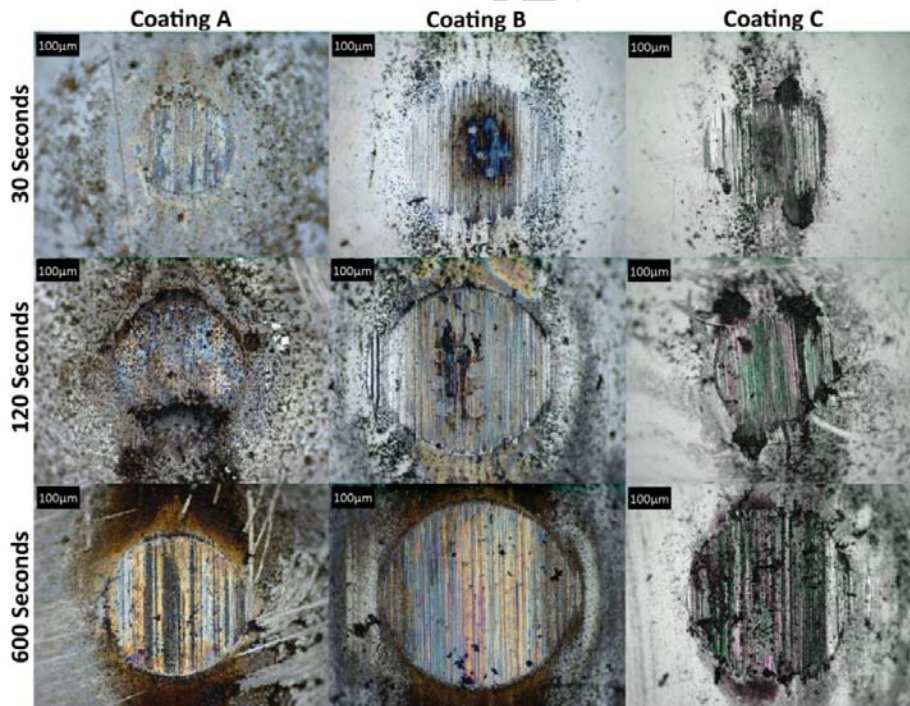
Figure 4: Photographs of 52100 balls after sliding against coatings A, B, and C, for varying test times.

Variability in wear scar diameter between coating A and coating C at 600 seconds is due to variance

between test runs, and does not accurately reflect that they showed similar wear depths.

Figure 4 shows no visual evidence of tribochemical reactions for coating A after 30 seconds and this coincides with the high coefficient of friction observed in the sliding tests. After 120 seconds, a large deposit of wear debris is seen in the contact. Tests that ran for 600 seconds show that a transfer layer has formed in the contact, and contact potential measurements show the presence of non-conducting material in the contact. The photographs clearly show abrasive grooves present on the steel surface, as well as a shearing of worn debris from the contact region, at the top and bottom of the image. The growth of a transfer layer is responsible for the reduction in friction during this initial stage. Similar abrasive grooves are evident on the surface of the ball when tested against coating B for all test times, and the shearing of worn debris from the contact is clearly evident after 600 seconds. A thick and stable transfer layer is unable to grow, however low friction is maintained by shear of the transfer layer in the contact.

It is important to recognise the type of interfacial motion that occurs in a tribo-contact. Scharf and Singer [20] describe the dynamics of transfer layer growth in terms of interfacial sliding, or shear. Based upon observations using the optical microscope, it appears that the transfer layer for coating C is stable, and an interfacial sliding mechanism is the dominant type of interfacial motion. There is little evidence of shearing of worn material from the contact region, the coefficient of friction has a low variance, and the debris in the contact appears thick and constant throughout the tests. For coatings A and B, the dominant interfacial mechanism appears to be shear of the transfer layer, potentially followed by circulation and re-attachment of the wear debris. Some transfer layer is present on the steel counterface even in the case of shear.

For all coatings, a gradual increase in friction was observed, and related to oxidation of the wear debris. For coatings A and B, higher friction was observed in general, and the increase in friction was followed by a gradual decrease in friction that can be related to the shear and loss of material from the interface. Due to the static nature of the transferred material on the surface of Coating C, a low and steady coefficient of friction was observed throughout the test, since no additional energy was required to shear wear debris in the contact.

Importantly, the wear depth of the DLC coatings can be related to the type of interfacial motion of the transfer layer. In the case of coatings A and B, shear of the wear debris from the steel surface reduces the protective ability of the transfer layer. As a result the coatings show increased wear, most likely by a three-body wear mechanism. The stability of the transfer layer on the ball surface for coating C protects the DLC coating.
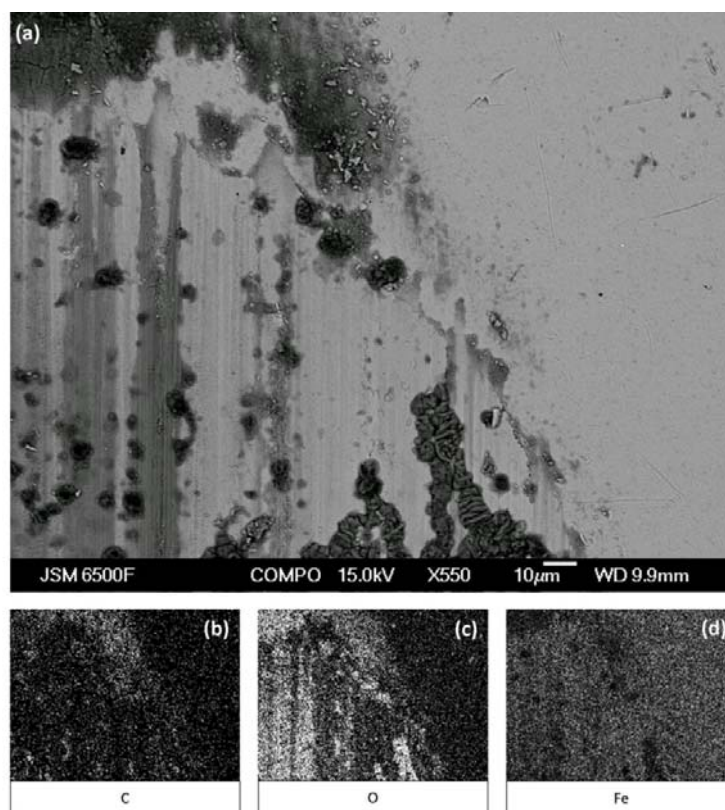
Figure 5: (a) BEI of 52100 steel ball after sliding against coating C for 600 seconds, and EDX maps showing

(b) carbon (c) oxygen, and (d) iron distributions on the surface.

Backscatter Electron Imaging (BEI) and Electron Dispersive X-ray (EDX) spectroscopy were used to study the species present at the interface. When using BEI, elements with a higher atomic number are shown to be brighter than those with a low atomic number. Figure 5 shows a BEI for the transferred material after sliding against coating C for 600 seconds. The debris appears darker in colour than the steel ball. Analysis of the debris using EDX analysis shows the presence of carbon and oxygen in the wear debris.

3.2. Raman spectroscopy of transfer layers

Raman spectroscopy was used to determine the chemical interactions that occur in the contact, and how they vary throughout the test for a steel ball versus a DLC coating in distilled water. Figure 6 shows the Raman spectra of the as-deposited DLC coatings. Typically, Raman spectra for DLC comprise of two carbon peaks at around 1580 cm^{-1} and 1330 – 1380 cm^{-1}, called the G-peak and D-peak respectively [26, 27]. These peaks often show changes in position and intensity based upon structural changes. The G-peak is related to the bonding and stretching of sp^2 bonded atoms. The D-peak arises from breathing modes of sp^2 bonded atoms in six fold

14

aromatic rings, and is observed only in the presence of disorder. The I(D)/I(G) ratio measures the degree of disorder within a graphitic layer. This ratio increases as changes in bonding occur.

Coating A has the highest I(D)/I(G) ratio, at 0.83. This is to be expected due to the higher percentage of sp^2 bonding in this sputtered DLC coating. Coatings B shows the lowest I(D)/I(G) ratio at 0.73 compared to 0.77 for coating C. Coatings B and C were both deposited via a PECVD process, and an approximate relationship exists between sp^3 content and I(D)/I(G) ratio [26]. The sp^3 content of both these coatings can be estimated at 35 – 50 %.
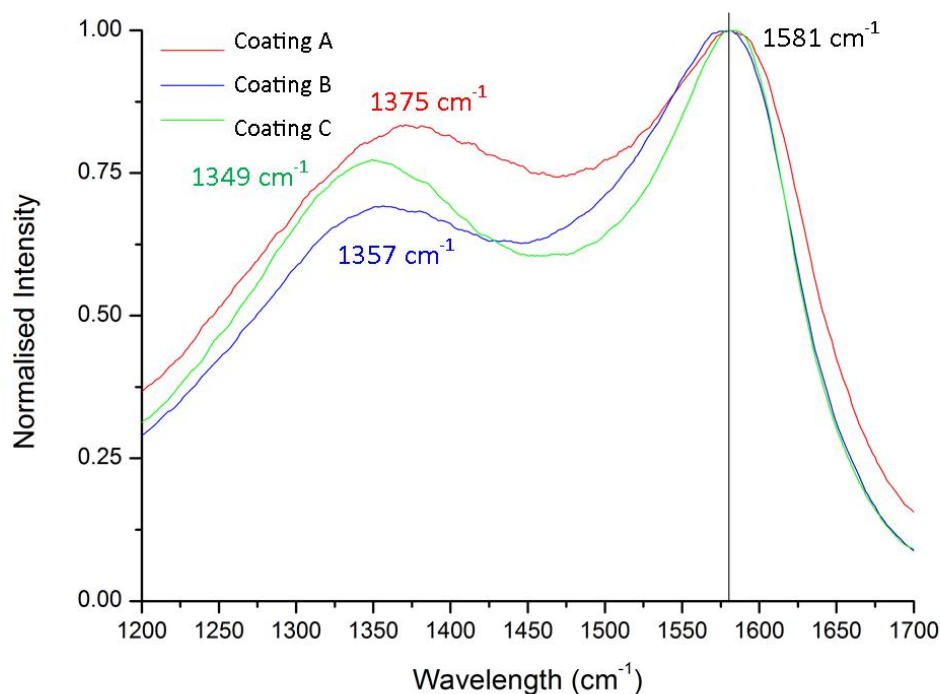
Figure 6: Raman spectra for coatings A, B, and C.

Raman spectra of the transfer layers formed when the DLC coatings wore against 52100 steel balls in distilled water are shown in Figure 7 after 30 seconds, 120 seconds, 600 seconds, and 3600 seconds of sliding wear. For each coating, two typical spectra are shown to more fully represent the surface state since a large degree of inhomogeneity was noted. Figure 7 (d) shows typical Raman spectra of magnetite (Fe_3O_4), maghemite (γ-Fe_2O_3), and hematite (α-Fe_2O_3) [28, 29].

The spectrum for the transfer layer from coating A after 30 seconds is mostly comprised of worn debris from the DLC coating. Using optical microscopy it was difficult to see any wear debris on the ball during this high

friction period. Adhesive forces would cause wear to the DLC coating, resulting in reaction of carbon with oxygen and water molecules by the mechanism of Li et al. [4]. The other peaks in the spectra, around 310 cm^{-1}, 532 cm^{-1}, and 667 cm^{-1} are due to magnetite (Fe_3O_4), which forms on the steel surface.

After 120 seconds, the spectra showed more evidence of magnetite, as well as peaks at 227 cm^{-1}, 245 cm^{-1}, 293 cm^{-1}, 414 cm^{-1}, 497 cm^{-1}, 612 cm^{-1} and 1321 cm^{-1}, which relate to those of hematite (α-Fe_2O_3). The highest peak of hematite overlays with the D-peak of a DLC coating, meaning it is difficult to observe the change in I(D)/I(G) ratio as the test progresses. After a 3600 seconds test, the Raman spectra potentially shows the presence of maghemite (γ-Fe_2O_3), characterised by the double peak at 660 (710) cm^{-1}. Magnetite and maghemite share peaks around 600cm^{-1} meaning it is difficult to distinguish between these.

As the test time increased for coating A, we observe a decrease in the intensity of the carbon peaks, and an increase in the intensity of the iron oxides present. This suggests that as the test continues, the interface is composed of less carbonaceous species and a higher proportion of iron oxide species. The shear of wear debris from the contact region has been observed for coating A by optical microscopy. The Raman spectra tell us that as the test continues there is less carbon present at the interface, and iron oxide species formed through wear of the ball are dominant. Magnetite is brittle and can easily be sheared, however hematite is a hard iron oxide and had an abrasive nature [30]. As a result of this, increased wear occurs to the DLC surface by a three-body mechanism involving the iron oxide wear particles.

Coating B shows a similar trend to coating A. There is initially a large volume of carbon on the ball surface, as seen from the high intensity of the spectra in Figure 7 (b), but this is removed from the contact as the test continues. Loss of the carbonaceous transfer layer leads to a three-body abrasive action between the contacting surfaces, increasing wear to both surfaces.

The spectra for coating C, in Figure 7 (c), show the presence of carbon at the interface is constant at all test times. Magnetite and hematite is also observed. These findings are in contrast to coatings A and B, and can be linked to the stability of the transfer layer on the ball surface. The transfer layer present here acts as a sacrificial layer to protect the surfaces from abrasive wear. In addition, the lack of evidence of shear suggests any iron oxide formed will not lead to the three-body abrasion that would occur in the case of shear. For this reason, coating C shows a low specific wear rate in comparison to the other coatings.
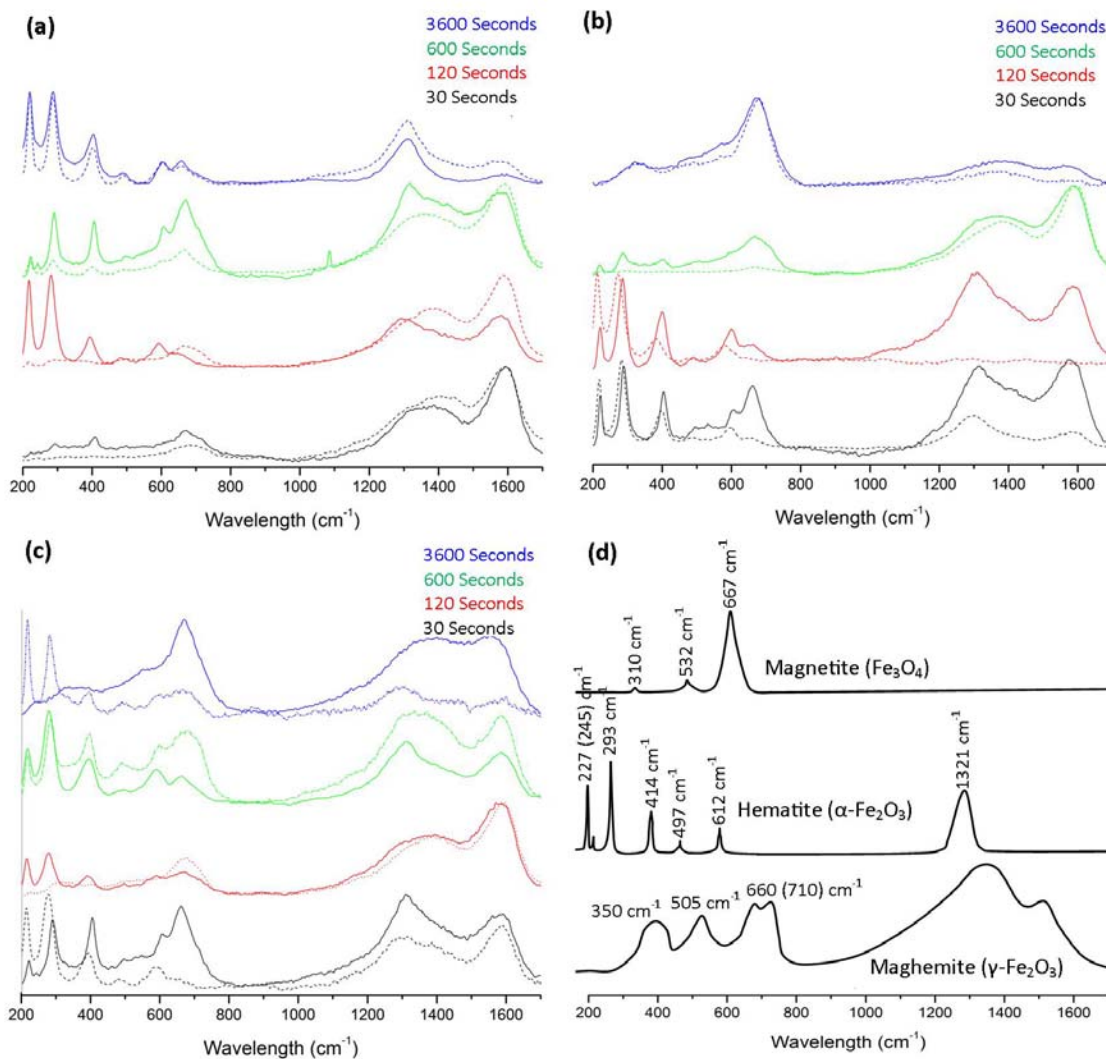
Figure 7: Raman spectra for transfer layers sliding against (a) coating A, (b) coating B, (c) coating C, after 30, 120, 600, and 3600 seconds test time. (d) Raman spectra of magnetite, hematite, and maghemite [28, 29]. In each case, two spectra from different locations on the ball surface are shown (by solid and dotted lines) to represent the inhomogeneity of the transfer layer.

In a general case, interfacial sliding will occur due to the stability of a transfer layer on the surface of a counterface. This might be due to increased shear strength of the transferred material, a lower roughness of the DLC surface, or alternate contact conditions. The Raman spectra presented show clearly the increased presence of carbon at the interface during interfacial sliding for coating C.

Previously, the presence of magnetite during the oxidation of steels in water has been linked to higher speeds and temperatures than α-Fe$_2$O$_3$ [22]. Also, the transition of magnetite to maghemite to hematite is well

established under sufficiently high temperature or pressure, by the reaction in Equation 6 [31]. In this work, no firm conclusions can be presented regarding the type of iron oxide on the surface and its correlation to test conditions. This is partially due to the inhomogeneity of the transfer layer.

$$Fe_3O_4 \xrightarrow{200°C} \gamma - Fe_2O_3 \xrightarrow{400°C} \alpha - Fe_2O_3 \tag{6}$$
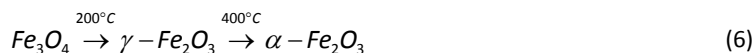
The Raman spectra provide us with a new insight into the dynamics between the chemical species present at the interface between a steel ball and a DLC coating during water-lubricated reciprocating sliding wear. The well-established carbonaceous transfer layer is shown to be unstable in some instances, instead replaced by an iron oxide layer. The tribological behaviour in terms of coefficient of friction and wear rate, and the volume of carbon at the interface, are related to the stability of the transfer layer. Interfacial sliding is the preferred mechanism, since shearing of the transfer layer causes a loss of carbon leading to increased wear rates.

3.3. Friction model

We consider that the coefficient of friction will vary as a function of the chemistry at the interface, and proportionally to the volume of debris in the contact region (or in this case, proportional to transfer layer thickness). Experimentally, we have shown that shear of the transfer layer from the region occurs in line with a decreasing coefficient of friction. An increase in the coefficient of friction is observed initially, as wear debris from the steel ball and the DLC coating react with oxidative species from the water environment.

Figure 8 (a) shows the experimental data fitted to the modified Elovich adsorption model (Equation 5) for coating C. Prediction intervals are fitted assuming normalised residuals at 95% confidence. Initially, the coefficient of friction is controlled by the changes in interfacial chemistry as gaseous species adsorb to the wear debris in the contact region. After approximately 800 seconds, the coefficient of friction reaches a local maximum and gradual wear of the oxidised debris from the region becomes the dominant factor, causing a subsequent decrease in the coefficient of friction. The change in percentage adsorbate over time can be seen in Figure 8 (b). Since it is the percentage adsorbate it is limited to a maximum value of 1.

The coefficient of friction modelled for coating A is compared to experimental measurements in Figure 9 (a). The initial rise in friction is excluded, since this is due to the composition of the coating. A steep decline in the coefficient of friction is observed after 2500 seconds. The assumptions of the model suggest that the volume

of wear debris in the interface is linked linearly with the decline in the coefficient of friction. Shear of the transfer layer from the region results in a steep decrease in the friction coefficient comparative to coating C. Figure 9 (b) shows how the percentage adsorbate changes over time. The rate of adsorption is much slower than in the case of coating C. The Elovich model for coating B is presented in Figure 10. As for coating B, a steep decline in the coefficient of friction occurs as the carbonaceous transfer layer is lost from the contact region.

For each model, the rate constant α should be of a similar value, since this defines the rate of oxidation of the wear debris. The roughness and hardness of the coatings will cause some variance in this value, but otherwise it should remain approximately the same in all tests. In this case, we found $\alpha = 3.41 \pm 0.2$ gave a good fit for all coatings. The initial rate of reaction β is of order 10^{-4} in good comparison to Borodich et al. [8].
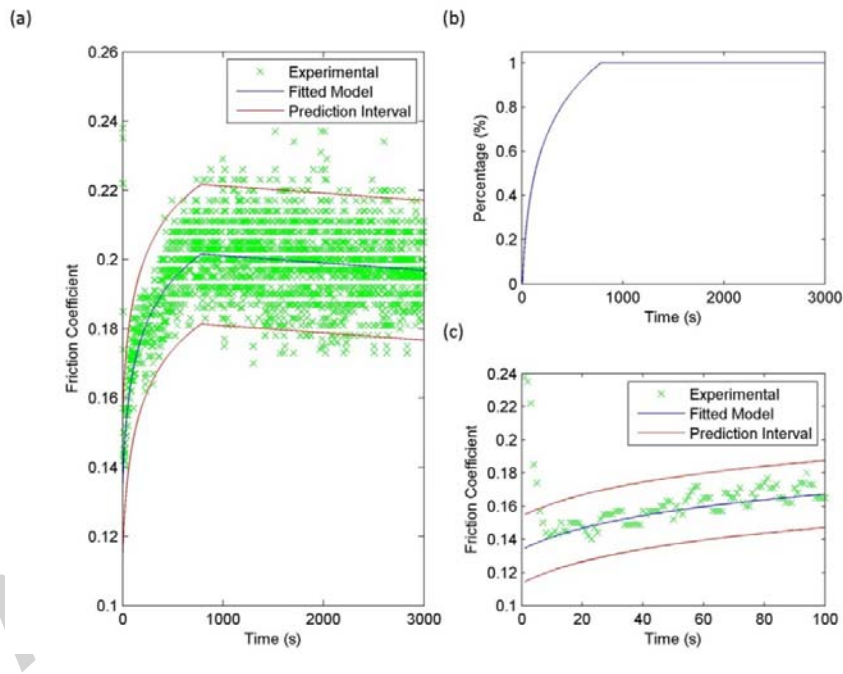
Figure 8: (a) Experimental friction data fitted to Elovich model for coating C for $\alpha = 3.35$ and $\beta = 0.011$. (b) Percentage adsorbance of oxidative species with time. (c) Deviation of coefficient of friction from model.
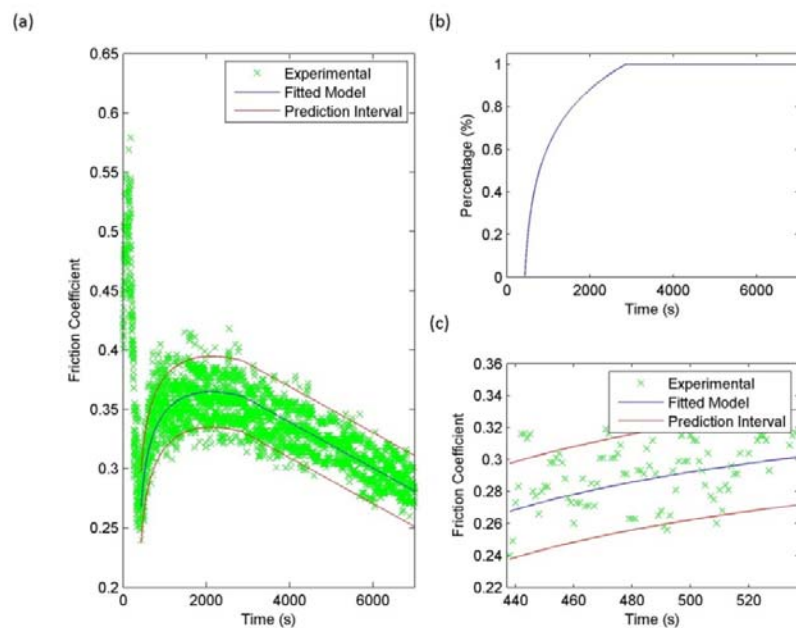
Figure 9: (a) Experimental friction data fitted to Elovich model for coating A for α = 3.57 and β = 0.004. (b) Percentage adsorbance of oxidative species with time. (c) Deviation of coefficient of friction from model.
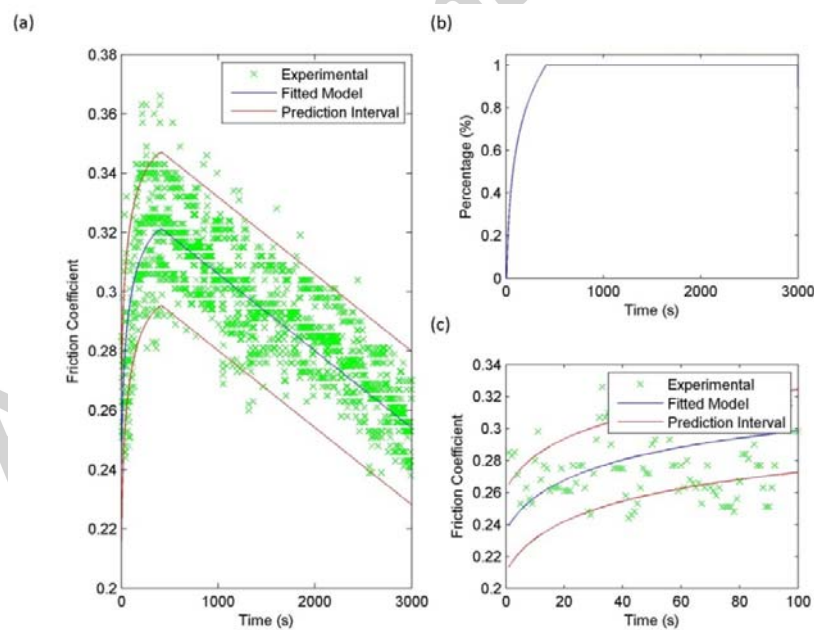
Figure 10: (a) Experimental friction data fitted to Elovich model for coating B for α = 3.33 and β = 0.020. (b) Percentage adsorbance of oxidative species with time. (c) Deviation of coefficient of friction from model.

The model confirms the dependence of the chemistry at the interface on the coefficient of friction. The initial increase in friction as the wear debris that makes up the transfer layer reacts with the environment is evident in the early stage. The rate of reaction is increased by plastic deformation and shear that occurs in the contact region, creating nascent surfaces with which polar species can react. Later in the friction tests, a gradual decline in the coefficient of friction is observed due to the loss of transfer layer from the interface by shear. For coatings A and B, a large proportion of transfer layer was sheared from the interface, and this is reflected in the steep decline in coefficient of friction. Coating C shows a more gradual decline due to the stability of the transfer layer on the ball surface. The coefficient of friction is lower overall for coating C, due to the interfacial sliding mechanism which is dominant.

4. Conclusion

The tribological properties of three DLC coatings were evaluated in distilled water, sliding against AISI 52100 steel balls. The frictional behaviour throughout the tests was varied. In all cases, a gradual increase in friction was observed, and linked to the oxidation of wear debris causing an increase in adhesion. For coating A and B, a subsequent decrease in friction was observed as the transfer layer was lost from the region. For coating C, low and stable friction was observed in long term behaviour due to an interfacial sliding mechanism between a stable transfer layer and the DLC coating. An Elovich-type adsorption model was used to accurately model the coefficient of friction throughout the test. Shear of the transfer layer from the region was included in the model in the form of a constant wear rate, resulting in a linear reduction in friction to match experimental observations.

For coatings A and B, Raman spectroscopy showed the increase in intensity of iron oxide species at the interface as the test time increased, replacing the carbonaceous transfer layer that was sheared from the contact. Coating C showed a carbonaceous transfer layer throughout the test, resulting in a low and steady coefficient of friction.

The wear to coating C was immeasurable, in contrast to coating A and B which showed specific wear rates of 1.7 mm^3/Nm and 2.2 x 10^{-6} mm^3/Nm. This was linked to the growth and decay of the transfer layer. Shear of the transfer layer from the contact region was observed for coatings A and B, whereas coating C showed a thick and stable transfer layer. The higher wear rate for coatings A and B was suggested to be due to a three-

body abrasive wear mechanism involving hard iron oxide particles. Coating C showed little evidence of shear and a lower wear rate as a result.

Further tests need to be performed in order to draw conclusions from the presence of hematite and magnetite at the interface. Variations in contact pressure and sliding speed could influence the distribution of species at the interface, and influence the tribological properties as a result. Of particular importance is further study to understand under what conditions interfacial sliding will occur, and under what conditions shear will be observed followed by wear to the DLC coating.

5. Acknowledgements

6. References

[1] C. Donnet, Recent progress on the tribology of doped diamond-like and carbon alloy coatings: a review, Surf Coat Tech, 100 (1998) 180-186.

[2] A. Erdemir, C. Donnet, Tribology of diamond-like carbon films: recent progress and future prospects, J Phys D Appl Phys, 39 (2006) R311-R327.

[3] J. Robertson, Diamond-like amorphous carbon, Mat Sci Eng R, 37 (2002) 129-281.

[4] H.X. Li, T. Xu, C.B. Wang, J.M. Chen, H.D. Zhou, H.W. Liu, Friction-induced physical and chemical interactions among diamond-like carbon film, steel ball and water and/or oxygen molecules, Diam. Relat. Mat., 15 (2006) 1228-1234.

[5] J. Andersson, R.A. Erck, A. Erdemir, Frictional behavior of diamondlike carbon films in vacuum and under varying water vapor pressure, Surf Coat Tech, 163 (2003) 535-540.

[6] A. Erdemir, The role of hydrogen in tribological properties of diamond-like carbon films, Surf Coat Tech, 146 (2001) 292-297.

[7] J.R. Jiang, S. Zhang, R.D. Arnell, The effect of relative humidity on wear of a diamond-like carbon coating, Surf Coat Tech, 167 (2003) 221-225.

[8] F.M. Borodich, L.M. Keer, Modeling effects of gas adsorption and removal on friction during sliding along diamond-like carbon films, Thin Solid Films, 476 (2005) 108-117.

[9] F.M. Borodich, C.S. Korach, L.M. Keer, Modeling the tribochemical aspects of friction and gradual wear of diamond-like carbon films, J Appl Mech-T Asme, 74 (2007) 23-30.

[10] J.A. Heimberg, K.J. Wahl, I.L. Singer, A. Erdemir, Superlow friction behavior of diamond-like carbon coatings: Time and speed effects, Appl Phys Lett, 78 (2001) 2449-2451.

[11] H. Zaidi, D. Paulmier, J. Lepage, The Influence of the Environment on the Friction and Wear of Graphitic Carbons .2. Gas Coverage of Wear Debris, Appl Surf Sci, 44 (1990) 221-233.

[12] P.L. Dickrell, N. Argibay, O.L. Eryilmaz, A. Erdemir, W.G. Sawyer, Temperature and Water Vapor Pressure Effects on the Friction Coefficient of Hydrogenated Diamondlike Carbon Films, J. Tribol.-Trans. ASME, 131 (2009) 5.

[13] P.L. Dickrell, W.G. Sawyer, A. Erdemir, Fractional coverage model for the adsorption and removal of gas species and application to superlow friction diamond-like carbon, J. Tribol.-Trans. ASME, 126 (2004) 615-619.

[14] P.L. Dickrell, W.G. Sawyer, J.A. Heimberg, I.L. Singer, K.J. Wahl, A. Erdemir, A gas-surface interaction model for spatial and time-dependent friction coefficient in reciprocating contacts: Applications to near-frictionless carbon, J. Tribol.-Trans. ASME, 127 (2005) 82-88.

[15] S.J. Park, K.R. Lee, D.H. Ko, Tribochemical reaction of hydrogenated diamond-like carbon films: a clue to understand the environmental dependence, Tribology International, 37 (2004) 913-921.

[16] M. Uchidate, H. Liu, A. Iwabuchi, K. Yamamoto, Effects of water environment on tribological properties of DLC rubbed against stainless steel, Wear, 263 (2007) 1335-1340.

[17] H. Ronkainen, Holmberg, K., Environmental and Thermal Effects on the Tribological Performance of DLC Coatings, in: A.D. Erdemir, C. (Ed.) Tribology of Diamond-Like Carbon Films, Springer, 2008, pp. 155 - 200.

[18] M.N. Gardos, Tribology and Wear Behaviour of Diamond, in: K.E.D. Spear, J. P. (Ed.) Synthetic Diamond: Emerging CVD Science and Technology, Wiley, New York, 1994, pp. 419 -

[19] X. Wu, T. Ohana, A. Tanaka, T. Kubo, H. Nanao, I. Minami, S. Mori, Tribochemical investigation of DLC coating in water using stable isotopic tracers, Appl Surf Sci, 254 (2008) 3397-3402.

[20] T.W. Scharf, I.L. Singer, Third Bodies and Tribochemistry of DLC Coatings, in: A.D. Erdemir, C. (Ed.) Tribology of Diamond-Like Carbon Films, Springer, 2008, pp. 201-236.

[21] S.J. Cho, K.R. Lee, K.Y. Eun, J.H. Hahn, D.H. Ko, Determination of elastic modulus and Poisson's ratio of diamond-like carbon films, Thin Solid Films, 341 (1999) 207-210.

[22] I.M. Hutchings, Tribology: Friction and Wear of Engineering Materials, Edward Arnold, 1992.

[23] H. Ronkainen, S. Varjus, K. Holmberg, Tribological performance of different DLC coatings in water-lubricated conditions, Wear, 249 (2001) 267-271.

[24] T.W. Scharf, I.L. Singer, Role of the Transfer Film on the Friction and Wear of Metal Carbide Reinforced Amorphous Carbon Coatings During Run-in, Tribol Lett, 36 (2009) 43-53.

[25] J. Fontaine, C. Donnet, A. Grill, T. LeMogne, Tribochemistry between hydrogen and diamond-like carbon films, Surf Coat Tech, 146 (2001) 286-291.

[26] A.C. Ferrari, J. Robertson, Raman spectroscopy of amorphous, nanostructured, diamond-like carbon, and nanodiamond, Philos T R Soc A, 362 (2004) 2477-2512.

[27] G. Irmer, A. Dorner-Reisel, Micro-Raman studies on DLC coatings, Adv Eng Mater, 7 (2005) 694-705.

[28] D.L.A. deFaria, S.V. Silva, M.T. deOliveira, Raman microspectroscopy of some iron oxides and oxyhydroxides, J Raman Spectrosc, 28 (1997) 873-878.

[29] S.J. Oh, D.C. Cook, H.E. Townsend, Characterization of iron oxides commonly formed as corrosion products on steel, Hyperfine Interact, 112 (1998) 59-65.

[30] K.J. Chin, H. Zaidi, T. Mathia, Oxide film formation in magnetized sliding steel/steel contact - analysis of the contact stress field and film failure mode, Wear, 259 (2005) 477-481.

[31] Y. Goto, The Effect of Squeezing on the Phase Transformation and Magnetic Properties of γ-Fe2O3, Jpn. J. Appl. Phys., 3 (1964) 739-744.